

Binding of Tetracycline and Chlortetracycline to the Enzyme Trypsin: Spectroscopic and Molecular Modeling Investigations

Zhenxing Chi, Rutao Liu*, Hongxu Yang, Hengmei Shen, Jing Wang

Shandong Provincial Key Laboratory of Water Pollution Control and Resource Reuse, School of Environmental Science and Engineering, Shandong University, China-America CRC for Environment and Health, Shandong Province, Jinan, People's Republic of China

Abstract

Tetracycline (TC) and chlortetracycline (CTC) are common members of the widely used veterinary drug tetracyclines, the residue of which in the environment can enter human body, being potentially harmful. In this study, we establish a new strategy to probe the binding modes of TC and CTC with trypsin based on spectroscopic and computational modeling methods. Both TC and CTC can interact with trypsin with one binding site to form trypsin-TC (CTC) complex, mainly through van der Waals' interactions and hydrogen bonds with the affinity order: TC>CTC. The bound TC (CTC) can result in inhibition of trypsin activity with the inhibition order: CTC>TC. The secondary structure and the microenvironment of the tryptophan residues of trypsin were also changed. However, the effect of CTC on the secondary structure content of trypsin was contrary to that of TC. Both the molecular docking study and the trypsin activity experiment revealed that TC bound into S1 binding pocket, competitively inhibiting the enzyme activity, and CTC was a non-competitive inhibitor which bound to a non-active site of trypsin, different from TC due to the Cl atom on the benzene ring of CTC which hinders CTC entering into the S1 binding pocket. CTC does not hinder the binding of the enzyme substrate, but the CTC-trypsin-substrate ternary complex can not further decompose into the product. The work provides basic data for clarifying the binding mechanisms of TC (CTC) with trypsin and can help to comprehensively understanding of the enzyme toxicity of different members of tetracyclines *in vivo*.

Citation: Chi Z, Liu R, Yang H, Shen H, Wang J (2011) Binding of Tetracycline and Chlortetracycline to the Enzyme Trypsin: Spectroscopic and Molecular Modeling Investigations. PLoS ONE 6(12): e28361. doi:10.1371/journal.pone.0028361

Editor: Hendrik W. van Veen, University of Cambridge, United Kingdom

Received: June 16, 2011; **Accepted:** November 7, 2011; **Published:** December 19, 2011

Copyright: © 2011 Chi et al. This is an open-access article distributed under the terms of the Creative Commons Attribution License, which permits unrestricted use, distribution, and reproduction in any medium, provided the original author and source are credited.

Funding: The work is supported by National Nature Science Foundation of China (NSFC, 20875055), the Cultivation Fund of the Key Scientific and Technical Innovation Project, Shanghai Tongji Gao Tingyao Environmental Science & Technology Development Foundation (STGEF), Graduate Independent Innovation Foundation of Shandong University (yzc10056) and Ministry of Education of China (708058) are also acknowledged. The funders had no role in study design, data collection and analysis, decision to publish, or preparation of the manuscript.

Competing Interests: The authors have declared that no competing interests exist.

* E-mail: rutaoliu@sdu.edu.cn

Introduction

Tetracycline (TC) and chlortetracycline (CTC) (structure with atom numbers shown in Fig. 1) are common members of tetracyclines, widely used for disease control and as feed additive in livestock for several decades due to their great therapeutic values [1]. Similar to other antibiotics, they are excreted mostly as the parent compound, representing 50–80% of the applied dose [2]. The excreted tetracyclines can enter soils, surface and ground water, being a potential risk to human health [3]. The toxicity of tetracyclines residues in the environment including animal food [4], soils [5], and surface and groundwater [3], has attracted widespread attention [6].

The water-soluble globular protein, trypsin (EC 3.4.21.4, structure shown in Figure S1) is a proteolytic enzyme that is excreted by the pancreas into the small intestine and takes part in the digestion of food proteins and other biological processes [7]. However, intake of any contaminants is likely to affect the activity of the enzyme *in vivo*. Tetracyclines interfere with processes of secretion as well as synthesis of pancreatic protein in pigeons [8], has effect on the secretion kinetics of the rat exocrine pancreas and can lead to the decrease of trypsin level in male wistar rats [9,10].

The fact indicates that tetracyclines can enter the pancrea. So, they have potential to interact with trypsin to affect the structure and function of trypsin [11]. We have studied the binding of oxytetracycline (belonging to tetracyclines) with trypsin [12]. However, the interaction mechanism of the other common tetracyclines (TC and CTC) with trypsin has not been studied previously. In this work, the binding mechanisms of TC and CTC with trypsin were investigated by multispectroscopic techniques and molecular modeling methods. The study is helpful for comprehensive understanding of the enzyme toxicity of different members of tetracyclines *in vivo* and their toxicity assessment in the environment.

Results and Discussion

Characterization of the Binding Interactions of TC (CTC) with Trypsin by Fluorescence Measurements Based on the Elimination of the Inner Filter Effects

In this study, we eliminated the inner filter effect for all of the fluorescence and synchronous fluorescence results to obtain accurate data. The fluorescence intensity was corrected using the eq 1.

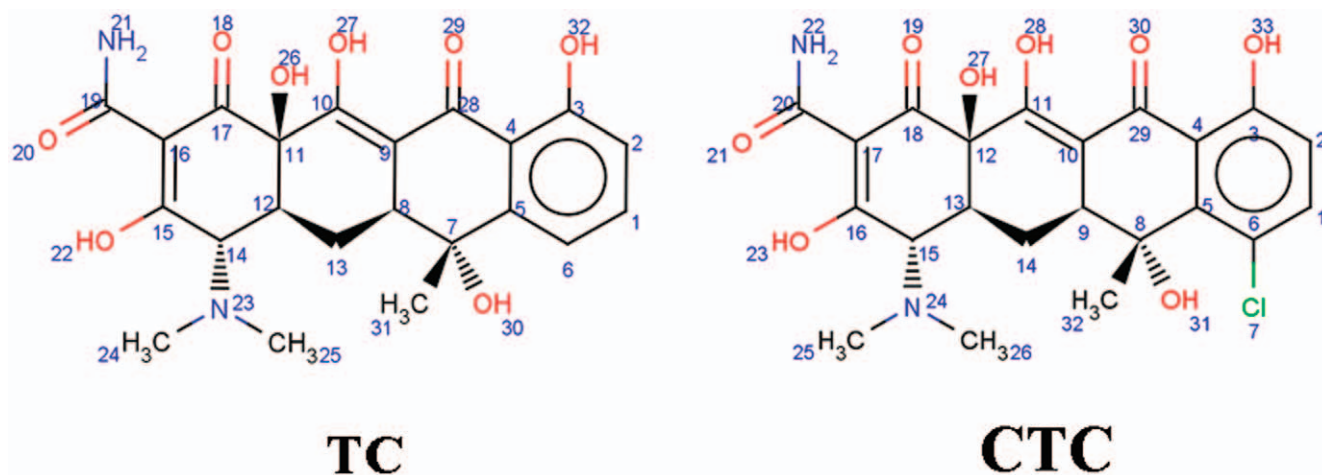


Figure 1. Molecular structure of TC and CTC (with atom numbers).
doi:10.1371/journal.pone.0028361.g001

Fluorescence spectra. The fluorescence intensity (F) of trypsin decreased regularly with increasing TC (CTC) concentrations (Figure 2A). Furthermore, a small blue shift was observed for the emission wavelengths, which suggests that the fluorescence chromophore of trypsin was placed in a more hydrophobic environment after the addition of TC (CTC) [13].

The fluorescence quenching data were analyzed according to the Stern-Volmer eq 2 to determine the quenching mechanism which can investigate whether TC (CTC) interact with trypsin to form trypsin-TC (CTC) complex. The Stern-Volmer plots for the quenching of trypsin by TC (CTC) at two different temperatures after correction are shown in Figure 2B. The K_{SV} and k_q at two different temperatures are listed in Table 1. The K_{SV} values decreased with increasing temperature and k_q was greater than $2.0 \times 10^{10} \text{ Lmol}^{-1} \text{ s}^{-1}$ [14,15]. These results indicate that the quenching was not initiated from dynamic collision but from the formation of a complex.

Binding parameters. The quenching mechanism was determined to be static quenching, so the binding constant (K_a) and the number of binding sites (n) can be calculated according to eq 3. A plot of $\log[(F_0-F)/F]$ vs $\log[\text{TC (CTC)}]$ yields $\log K_a$ as the intercept on the y axis and n as the slope (Figure S2). Table 2 shows the calculated K_a and n . The number of binding sites, n , is approximately 1, indicating that there is one binding site in trypsin for TC (CTC) during their interaction. The affinity order is as follows: TC > CTC.

Thermodynamic parameters and binding forces. The acting forces between small organic molecules and biomolecules include hydrogen bonds, van der Waals interactions, electrostatic forces and hydrophobic interaction forces. Because the temperature effect is very small, the interaction enthalpy change (ΔH°) can be regarded as a constant if the temperature range is not too wide. The enthalpy change (ΔH°), free-energy change (ΔG°) and the entropy change (ΔS°) for the interaction between TC (CTC) and trypsin were calculated according to the van't Hoff equation (eq 4) and thermodynamic equation (eq 5) (Table 2). The negative ΔH° and ΔS° indicated that van der Waals interactions and hydrogen bonds play the major role during the interaction. In addition, the negative sign of ΔG° indicates the binding of TC (CTC) with trypsin is spontaneous [14].

Energy transfer between TC (CTC) and trypsin. The overlap of the absorption spectrum of TC (CTC) with the fluorescence emission spectrum of trypsin is shown in Figure S3. According to Förster's nonradiative energy transfer theory [16],

the energy transfer will happen under the conditions: (i) the donor can produce fluorescence light; (ii) the absorption spectrum of the receptor overlaps enough with the donor's fluorescence emission spectrum; (iii) the distance between the donor and the acceptor is less than 8 nm.

It has been reported for trypsin that, $k^2 = 2/3$, $n = 1.336$ and $\Phi = 0.118$ [17]. \bar{J} in eq 8 was evaluated by integrating the UV absorption and fluorescence emission spectra (Figure S3). Based on these data and eq 6–9, the overlap integral \bar{J} , R_0 , E , and r can be evaluated (Table 3). The distance between TC (CTC) and the tryptophan residues in trypsin after interaction is lower than 8 nm. These accords with conditions of Förster's nonradiative energy transfer theory, indicating again the static quenching interaction (forming a complex) between TC (CTC) and trypsin.

In summary, Both TC and CTC can interact with trypsin through van der Waals' interactions and hydrogen bonds with one binding site to form a complex. The binding process is spontaneous.

Effect of TC (CTC) on Trypsin Activity

The effects of different concentrations of TC (CTC) on the activity of trypsin are presented in Figure 3. The trypsin activity decreased with increasing TC (CTC) concentrations. At a molar ratio of 120:1 (TC (CTC) to trypsin), the activity of trypsin decreased to only 48.3 and 19.6% of the initial level for TC and CTC, respectively. Both TC and CTC can inhibit trypsin activity with the inhibition order as follows: CTC > TC.

To confirm the inhibition mode, the lineweaver-burk plots of trypsin with and without TC and CTC were drawn (Figure 4). The lineweaver-burk plots for TC intersect on the vertical axis, showing a typical feature of competitive inhibition [18]. However, the lineweaver-burk plots with and without CTC intersect on the abscissa axis, which is the typical noncompetitive inhibition characteristic. The inhibition mechanisms were illustrated in Figure 4. TC binds to the active site of trypsin and hinders the binding of the enzyme substrate, leading to the enzyme inhibition. Although CTC binds to a non-active site of trypsin which does not hinder the binding of the enzyme substrate, the CTC-trypsin-substrate ternary complex can not further decompose into the product.

Computational Modeling of the Trypsin-TC (CTC) Complex

Both TC and CTC can interact with trypsin with one binding site to form trypsin-TC (CTC) complex. So we employed the

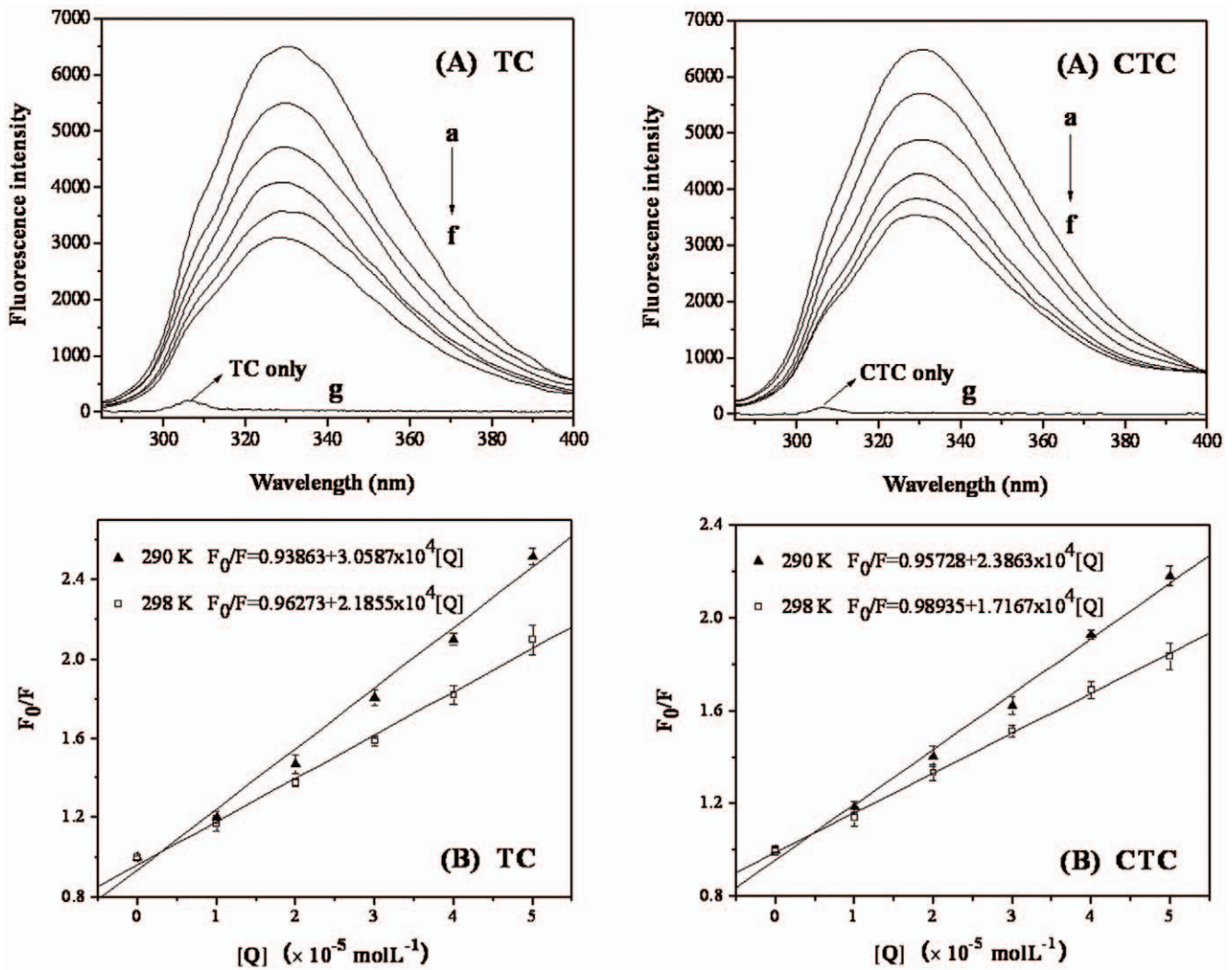


Figure 2. (A) Effect of TC (CTC) on trypsin fluorescence (corrected). (B) Stern-Volmer plots for the quenching of trypsin by TC and CTC at different temperatures (corrected). Data represent the mean \pm SD of three independent experiments. **Conditions:** (A) trypsin ($5 \times 10^{-6} \text{ mol L}^{-1}$) with different concentrations of TC and CTC ($\times 10^{-5} \text{ mol L}^{-1}$, a, 0; b, 1; c, 2; d, 3; e, 4; f, 5); g: TC (CTC) only, concentration $5 \times 10^{-5} \text{ mol L}^{-1}$; pH 7.6; T = 298 K. (B) trypsin concentration: $5 \times 10^{-6} \text{ mol L}^{-1}$; pH 7.6. doi:10.1371/journal.pone.0028361.g002

molecule docking method to find the specific binding site of TC (CTC) on trypsin. The crystal structure of trypsin was taken from the Protein Data Bank (entry PDB code 2ZQ1). The best energy ranked results are shown in Figure 5 and Figure 6.

Trypsin is serine protease, with the catalytic triad composed of His-57, Asp-102 and Ser-195, and the primary substrate-binding pocket (S1 binding pocket) formed by residues 189–195, 214–220 and 225–228 [19,20]. It can be shown in Figure 5 that TC binds into the S1 binding pocket, occupying the active site of the enzyme substrate. Hence, the trypsin activity is competitively inhibited by TC [21]. However, CTC does not bind into the S1 binding pocket. So the trypsin activity is noncompetitively inhibited. The computational modeling investigation further confirms the conclusions of the trypsin activity experiment.

For TC, hydrogen bonds exist between the hydrogen atom on the oxygen atom at position 30 of TC and the oxygen atoms on HIS 57 and SER 195, the oxygen atom at position 30 of TC and that on SER 195 (Figure 6). There are van der Waals interactions between the two hydrogen atoms on the nitrogen atom at position 21 of TC and the residue TRP 215. For CTC, there are hydrogen bonds between the oxygen atom at position 28 of CTC and the nitrogen atom on LYS 239 (Figure 6). The van der Waals interactions exist between the nitrogen atom on LYS 239 and the oxygen atoms at position 21 and position 23, the nitrogen atom at

Table 1. Stern-Volmer quenching constants for the interaction of TC (CTC) with trypsin at different temperatures.

T (K)	$K_{sv} (\times 10^5 \text{ L mol}^{-1})$	$k_q (\times 10^{12} \text{ L mol}^{-1} \text{ s}^{-1})$	R^a	S.D. ^b
TC 290	0.30587	3.0587	0.99518	0.06302
298	0.21855	2.1855	0.99701	0.03544
CTC 290	0.23863	2.3863	0.99674	0.04041
298	0.17167	1.7167	0.999	0.01604

^aR is the correlation coefficient.

^bS.D. is the standard deviation for the K_{sv} values.

doi:10.1371/journal.pone.0028361.t001

Table 2. Binding constants and relative thermodynamic parameters of the TC (CTC)-trypsin system.

T (K)	K_a ($\times 10^5$ L mol $^{-1}$)	n	R ^a	ΔH° (kJmol $^{-1}$)	ΔS° (Jmol $^{-1}$ K $^{-1}$)	ΔG° (kJmol $^{-1}$)
TC	290	1.8479	0.99935	-64.662	-122.32	-29.138
	298	0.8995	0.99976			-28.262
CTC	290	1.0383	0.99936	-52.64	-85.486	-27.849
	298	0.5778	0.9978			-27.165

^aR is the correlation coefficient for the K_a values.
doi:10.1371/journal.pone.0028361.t002

position 22 and the two hydrogen atoms on the nitrogen atom at position 22 of CTC. In addition, the modeled structure showed that hydrophobic interactions (TC with VAL 213, CTC with ILE 242) and other forces (TC with HIS 57, LEU 99, SER 190, GLN 192, SER 195, TRP 215 and CYS 220, and CTC with LEU 123, THR 125, LYS 204, LYS 239 and ILE 242) are also present. However, the hydrogen bonds and van der Waals interactions play a major role in the binding of TC and CTC to trypsin, in agreement with our conclusion of thermodynamic analysis (negative ΔH° and ΔS°).

From the docking result of TC with trypsin (Figure 5), we found that it is the benzene ring that first enters into the S1 binding pocket during its interaction with the enzyme. The molecular structure of CTC is the same as that of TC except the chlorine atom on the benzene ring (Figure 1). The Cl atom hinders CTC entering into the S1 binding pocket, resulting in its different binding site on trypsin and enzyme activity inhibition mechanism from TC.

Investigation of Trypsin Conformation Changes

UV-Vis absorption spectra studies. UV-vis absorption spectroscopy technique can be used to explore the structural changes of protein and to investigate protein-ligand complex formation. The UV-vis absorption spectra of trypsin in the presence and absence of TC (CTC) are shown in Figure 7. Trypsin has two absorption peaks. The strong absorption peak at about 206 nm reflects the framework conformation of the protein [22]. The weak absorption peak at about 274 nm appears to be due to the aromatic amino acids (Trp, Tyr and Phe) [23]. With gradual addition of TC (CTC) to trypsin solution, the intensity of the peak at 206 nm decreases and red shifts and the intensity of the peak at 274 nm also decreases. The results indicate that the interactions between TC (CTC) and trypsin leads to the loosening and unfolding of the protein skeleton and increases the hydrophobicity of the microenvironment of the aromatic amino acid residues [24].

Synchronous fluorescence. Synchronous fluorescence spectroscopy can give information about the molecular environment in the vicinity of chromophores. The spectrum is obtained through the simultaneous scanning of the excitation and emission monochromators while maintaining a constant wavelength interval between them. When the wavelength intervals ($\Delta\lambda$) are stabilized at 15 nm or 60 nm, the synchronous fluorescence gives the

characteristic information of tyrosine residues or tryptophan residues, respectively [25].

The synchronous fluorescence spectra of trypsin with various amounts of TC (CTC) in Figure 8A show that the emission peaks do not shift over the investigated concentration range, which indicates that TC (CTC) have little effect on the microenvironment of the tyrosine residues in trypsin. In Figure 8B, the emission maximum of the tryptophan residue shows a slight blue shift (from 276 to 275, 274.8 nm for TC and CTC, respectively) which indicates that the conformation of trypsin was changed such that the polarity around the tryptophan residues decreased and the hydrophobicity was increased [26].

Circular dichroism. To ascertain the possible influence of TC (CTC) binding on the secondary structure of trypsin, CD measurements were performed in the presence of different TC (CTC) concentrations (Figure 9). The estimates for the secondary structural elements found by the Jasco secondary structure manager software are listed in Table 4.

The CD spectrum of trypsin exhibits a negative band in the ultraviolet region at about 199 nm. The calculated secondary structure content of trypsin was 1.2% α -helix, 49.5% β -pleated sheet, 8.6% β -turn and 40.8% random coil. With the addition of TC (CTC), the intensity of the negative peak increased with blue shift for TC. However, the negative peak increased with red shift for CTC. At trypsin/TC ratio of 1:1, the α -helix increased by 0.5%, the β -pleated sheet decreased by 6.9%, and the β -turn increased by 7%. For CTC, the α -helix decreased by 0.7%, the β -pleated sheet increased by 5%, and the β -turn decreased by 3.8%, having reverse trend from that of TC. The bound CTC has opposite impact on the secondary structure content of trypsin compared to TC, because of the different binding site of TC and CTC on trypsin, in good accordance with the conclusion of the trypsin activity experiment and the molecule docking investigation.

As mentioned above, the binding of TC (CTC) can lead to the loosening and unfolding of the protein skeleton and increases the hydrophobicity of the microenvironment of the tryptophan residues of trypsin. The α -helix and the β -turn of the secondary structure of trypsin increased and the β -pleated sheet decreased because of bound TC. However, the bound CTC has reverse impact on the secondary structure content of trypsin compared to TC.

Table 3. Energy transfer parameters between TC (CTC) and trypsin.

Parameters	Overlap integral J (cm 3 L mol $^{-1}$)	Efficiency of transfer E	Critical distance R ₀ (nm)	Energy transfer distance r (nm)
TC	1.603×10^{-14}	0.0672	2.65	4.11
CTC	1.462×10^{-14}	0.0699	2.61	4.02

doi:10.1371/journal.pone.0028361.t003

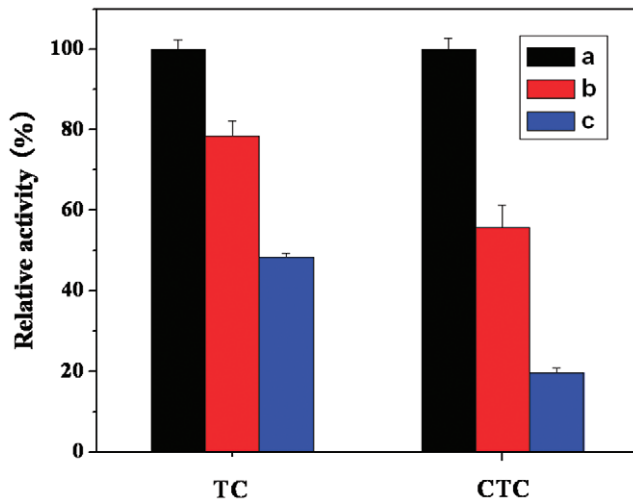


Figure 3. Effect of TC and CTC on the activity of trypsin. Data represent the mean \pm SD of three independent experiments. **Conditions:** trypsin (1.67×10^{-6} mol L⁻¹) with different concentrations of TC and CTC ($\times 10^{-5}$ mol L⁻¹, a, 0; b, 10; c, 20); pH 7.6; T=298 K. doi:10.1371/journal.pone.0028361.g003

Conclusions

In this paper, we simulated and compared the interaction of the widely used veterinary drug tetracyclines (TC and CTC) with trypsin. The experimental results indicate that both TC and CTC can interact with trypsin with one binding site mainly through van

der Waals interactions and hydrogen bonds with the affinity order: TC>CTC. TC bound into S1 binding pocket, competitively inhibiting the enzyme activity, and CTC was a non-competitive inhibitor which bound to a non-active site of trypsin, different from TC because of the Cl atom on the benzene ring of CTC which hinders CTC entering into the S1 binding pocket. CTC does not hinder the binding of the enzyme substrate, but the CTC-trypsin-substrate ternary complex can not further decompose into the product. The binding of TC (CTC) can also change the secondary structure and the microenvironment of the tryptophan residues of trypsin. However, CTC has opposite effect on the secondary structure content of trypsin from TC because of their different binding sites on trypsin. The established research route combing spectroscopic techniques and the molecular modeling method in the research is worth spreading to explore the binding mechanisms of other small organic pollutants and drugs.

Materials and Methods

Reagents

Trypsin (from bovine pancreas, Amresco) was dissolved in ultrapure water to form a 5×10^{-4} mol L⁻¹ solution, then preserved at 0–4°C and diluted as required. We prepared stock solutions of TC (1.0×10^{-3} mol L⁻¹) and CTC (1.0×10^{-3} mol L⁻¹) by dissolving 0.0481 g tetracycline hydrochloride (Sigma) and 0.0515 g chlortetracycline hydrochloride (Amresco) in 100 mL of water, respectively.

BAEE (N- α -benzoyl-L-arginine ethyl ester, from Sinopharm Chemical Reagent Co., Ltd., BR) was dissolved in ultrapure water to form a 1.0×10^{-2} mol L⁻¹ solution.

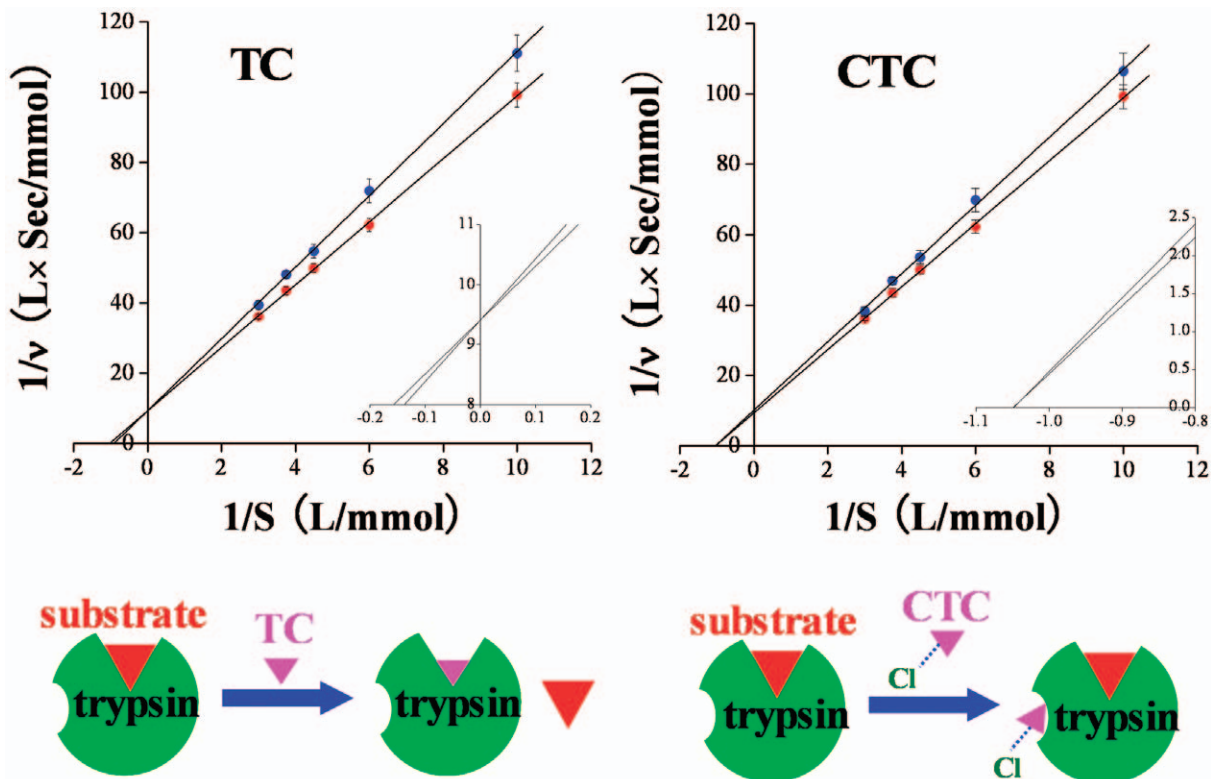


Figure 4. Lineweaver-Burk plots of trypsin in the presence (blue circle) and absence (red circle) of TC (CTC), and the schematic diagrams for the binding of TC and CTC with trypsin. Data represent the mean \pm SD of five independent experiments. **Conditions:** trypsin concentration: 1.67×10^{-6} mol L⁻¹; TC and CTC concentration: 3.33×10^{-5} mol L⁻¹; pH 7.6. doi:10.1371/journal.pone.0028361.g004

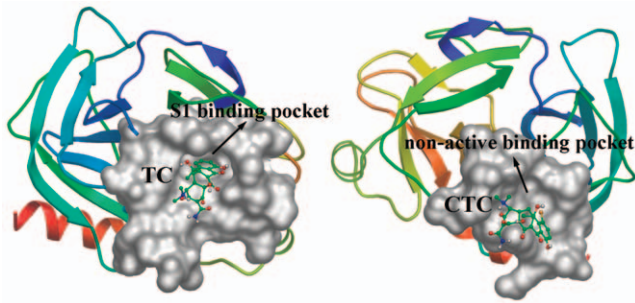


Figure 5. The binding mode between TC (CTC) and trypsin. Trypsin is shown in cartoon. The interacting side chains of trypsin are displayed in surface mode. TC and CTC are represented using balls and stick. The atoms of TC and CTC are color-coded as follows: O, red; N: blue; C, green; H, white.
doi:10.1371/journal.pone.0028361.g005

Phosphate buffer (0.2 mol L^{-1} , mixture of $\text{NaH}_2\text{PO}_4 \cdot 2\text{H}_2\text{O}$ and $\text{Na}_2\text{HPO}_4 \cdot 12\text{H}_2\text{O}$, pH 7.6) was used to control pH. $\text{NaH}_2\text{PO}_4 \cdot 2\text{H}_2\text{O}$ and $\text{Na}_2\text{HPO}_4 \cdot 12\text{H}_2\text{O}$ were of analytical reagent grade, obtained from Tianjin Damao Chemical Reagent Factory.

Apparatus and Methods

All fluorescence spectra were recorded on an F-4600 spectrofluorimeter (Hitachi, Japan). The excitation and emission slit widths were set at 5.0 nm. The scan speed was 1200 nm/min. PMT (photo multiplier tube) voltage was 800 V.

UV-visible absorption spectra were measured on a UV-2450 spectrophotometer (Shimadzu, Kyoto, Japan). CD spectra were recorded on a J-810 CD spectrometer (JASCO). The pH measurements were made with a pHs-3C acidity meter (Pengshun, Shanghai, China).

CD measurements. CD spectra were collected from 190 to 260 at 0.2 nm intervals on a JASCO J-810 CD spectrometer. Three scans were made and averaged for each CD spectrum. The protein conformation was computed using Yang.jwr software [27].

Fluorescence measurements. The fluorescence measurements were carried out as follows: to each of a series of 10 mL test tubes, 1.0 mL of 0.2 mol L^{-1} phosphate buffer (pH 7.6) and 1.0 mL of $5 \times 10^{-5} \text{ mol L}^{-1}$ trypsin were added, and then different amounts of $1.00 \times 10^{-3} \text{ mol/L}$ stock solution of TC and CTC were added. The fluorescence spectra were then measured

(excitation at 278 nm and emission wavelengths of 285–450 nm). The synchronous fluorescence spectra were measured at $\lambda_{\text{ex}} = 250 \text{ nm}$, $\Delta\lambda = 15 \text{ nm}$ and $\Delta\lambda = 60 \text{ nm}$.

To eliminate the inner filter effects of protein and ligand, absorbance measurements were performed at excitation and emission wavelengths of the fluorescence measurements. The fluorescence intensity was corrected using the equation [28]:

$$F_{\text{cor}} = F_{\text{obsd}} 10^{(A_1 + A_2)/2} \quad (1)$$

where F_{cor} and F_{obsd} are the corrected and observed fluorescence intensities, respectively; whereas A_1 and A_2 are the sum of the absorbance of protein and ligand at the excitation and emission wavelengths, respectively.

To confirm the quenching mechanism, the fluorescence quenching data were analyzed according to the Stern-Volmer equation [29]:

$$\frac{F_0}{F} = 1 + K_{\text{sv}}[Q] = 1 + k_q\tau_0[Q] \quad (2)$$

where F_0 and F are the fluorescence intensities in the absence and presence of the quencher, respectively. K_{sv} is the Stern-Volmer quenching constant, $[Q]$ is the concentration of the quencher, k_q is the quenching rate constant of the biological macromolecule and τ_0 is the fluorescence lifetime in the absence of quencher.

Binding parameters. For the static quenching interaction, when small molecules bind independently to a set of equivalent sites on a macromolecule, the binding constant (K_a) and the number of binding sites (n) can be determined by the following equation [30]:

$$\lg \frac{(F_0 - F)}{F} = \lg K_a + n \lg [Q] \quad (3)$$

where F_0 , F and $[Q]$ are the same as in eq 2, K_a is the binding constant, and n is the number of binding sites per trypsin molecule.

Thermodynamic parameters. If the enthalpy change (ΔH°) does not vary significantly over the temperature range studied, the enthalpy change (ΔH°), free-energy change (ΔG°) and the entropy change (ΔS°) can be calculated based on the van't Hoff equation (eq 4) and thermodynamic equation (eq 5):

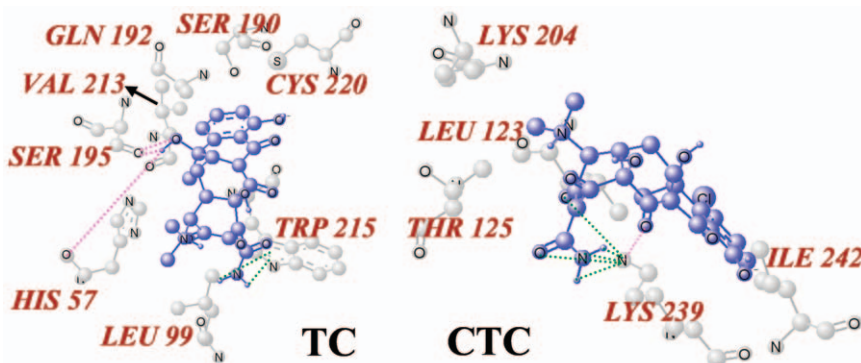


Figure 6. The molecular modeling of interaction between TC (CTC) and trypsin. The atoms of TC and CTC are marked with blue and the atoms of amino acid residues of trypsin are labeled with gray. The hydrogen bonds between TC (CTC) and trypsin are indicated by pink dashed line. The van der Waals interactions are illustrated with green dashed line.
doi:10.1371/journal.pone.0028361.g006

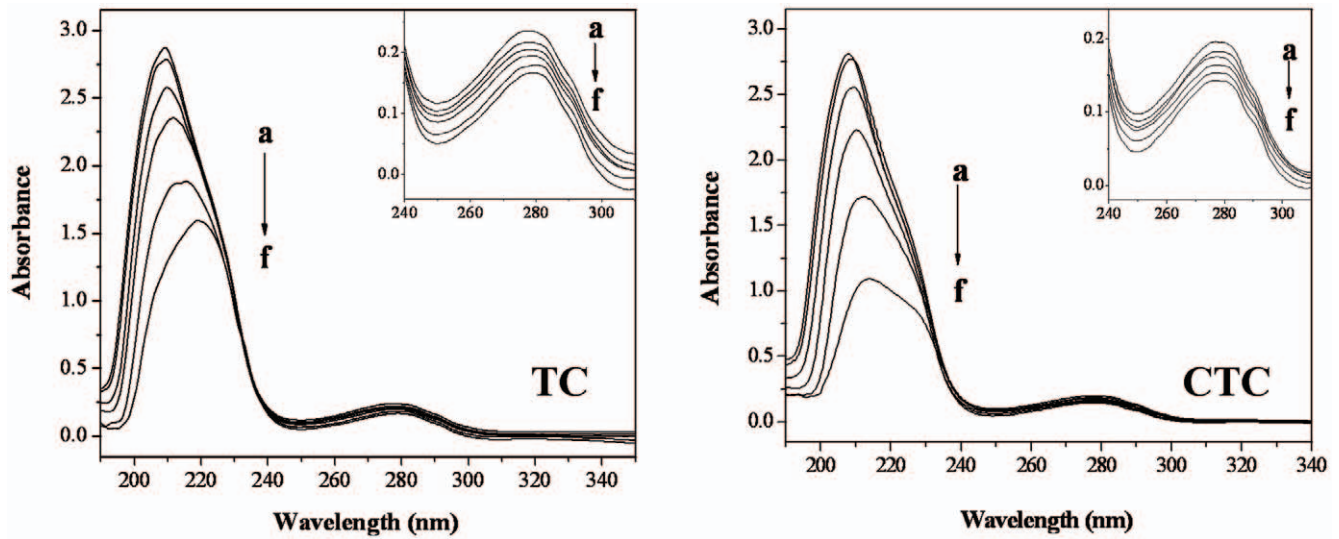


Figure 7. UV-vis spectra investigation. Conditions: trypsin (4×10^{-5} mol L⁻¹) with different concentrations of TC and CTC ($\times 10^{-5}$ mol L⁻¹, a, 0; b, 2; c, 6; d, 10; e, 15; f, 20) (vs the same concentration of TC (CTC) solution); pH 7.6; T = 298 K. doi:10.1371/journal.pone.0028361.g007

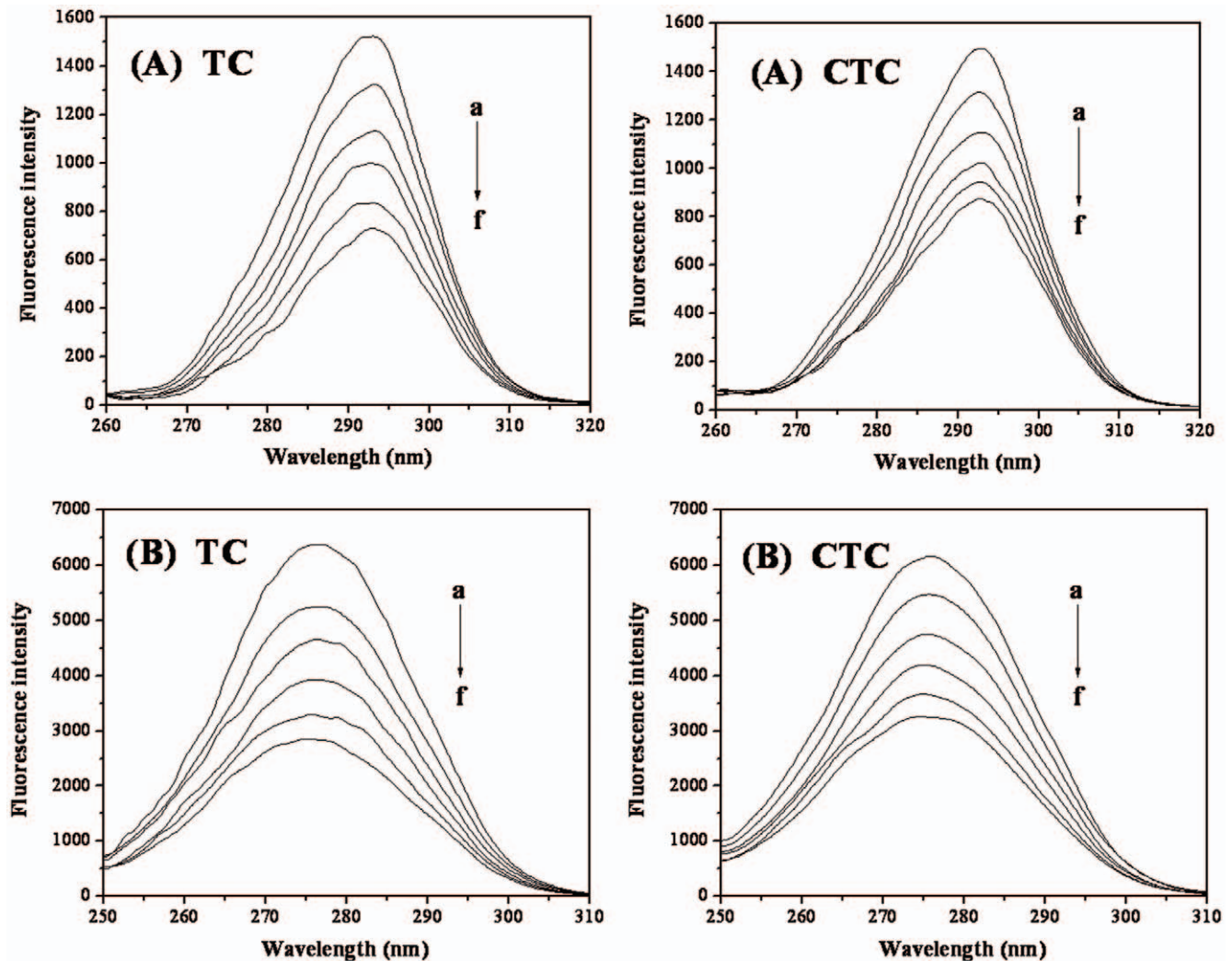


Figure 8. Synchronous fluorescence spectra of trypsin (corrected). (A) $\Delta\lambda = 15$ nm and (B) $\Delta\lambda = 60$ nm. Conditions: trypsin (5×10^{-6} mol L⁻¹) with different concentrations of TC and CTC ($\times 10^{-5}$ mol L⁻¹, a, 0; b, 1; c, 2; d, 3; e, 4; f, 5); pH 7.6; T = 298 K. doi:10.1371/journal.pone.0028361.g008

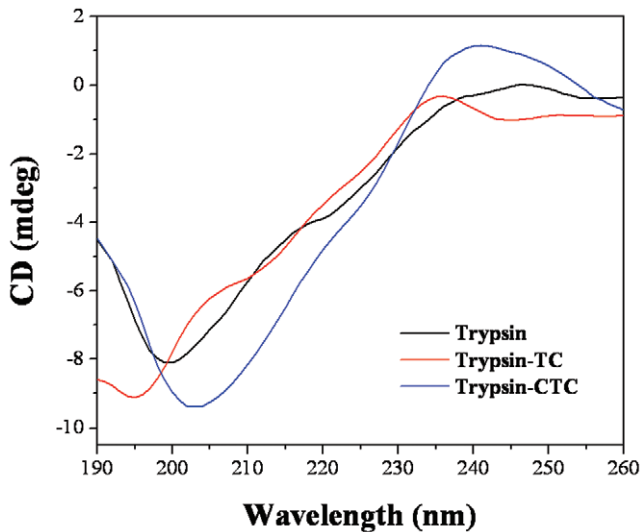


Figure 9. CD spectra of trypsin and the trypsin-TC (CTC) system at room temperature. Conditions: trypsin (5×10^{-5} mol L⁻¹) with 0 or 5×10^{-5} mol L⁻¹ TC (CTC); pH 7.6. doi:10.1371/journal.pone.0028361.g009

$$\ln\left(\frac{(K_a)_2}{(K_a)_1}\right) = \left(\frac{1}{T_1} - \frac{1}{T_2}\right) \left(\frac{\Delta H^\circ}{R}\right) \quad (4)$$

$$\Delta G^\circ = \Delta H^\circ - T\Delta S^\circ = -RT \ln K_a \quad (5)$$

where $(K_a)_1$ and $(K_a)_2$ are the binding constants at T_1 and T_2 and R is the universal gas constant.

Energy transfer calculation. According to the Förster's nonradiation energy transfer theory, the parameters related to energy transfer can be calculated based on the equations as follows.

The energy transfer effect is related not only to the distance between the acceptor and the donor but also to the critical energy transfer distance, that is:

$$E = \frac{R_0^6}{R_0^6 + r^6} \quad (6)$$

where r is the distance between the acceptor and the donor, R_0 is the critical distance when the transfer efficiency is 50%, which can be calculated by:

$$R_0^6 = 8.79 \times 10^{-25} K^2 n^{-4} \Phi J \quad (7)$$

where K^2 is the spatial orientation factor of the dipole, n is the refractive index of the medium, Φ is the fluorescence quantum yield of the donor, and J is the overlap integral of the fluorescence emission spectrum of the donor and the absorption spectrum of the acceptor,

$$J = \frac{\int_0^\infty F(\lambda)\varepsilon(\lambda)\lambda^4 d\lambda}{\int_0^\infty F(\lambda)d\lambda} \quad (8)$$

where $F(\lambda)$ is the fluorescence intensity of the fluorescence donor at wavelength λ and $\varepsilon(\lambda)$ is the molar absorption coefficient of the acceptor at wavelength λ . The energy transfer efficiency is given by

$$E = 1 - \frac{F}{F_0} \quad (9)$$

where F_0 and F are the same in eq 2.

Trypsin activity determination. The activity of trypsin was measured using BAEE as the substrate. Trypsin can catalyze BAEE into N-benzoyl-L-arginine. The UV absorption intensity of BAEE is far weaker than that of N-benzoyl-L-arginine. The enzyme activity was obtained based on the increase in absorbance at 253 nm in 2.0×10^{-2} mol L⁻¹ phosphate buffer (mixture of NaH₂PO₄·2H₂O and Na₂HPO₄·12H₂O, pH 7.6) containing 3.0×10^{-4} mol L⁻¹ BAEE before and after the addition of trypsin (concentration given in the legend of figure 3 and 4) [31].

The velocity of the enzymatic reaction (v , mmol L⁻¹ S⁻¹) was calculated using the following equation:

$$v = \frac{2 \times A_{253nm}}{\varepsilon \times 10^{-3} \times 60} \quad (10)$$

where A_{253nm} is the absorbance of the reaction system within 0.5 min, deducted the absorbance of TC and CTC when they exist in the system. ε is the molar extinction coefficient of BAEE.

Molecular modeling study. Docking calculations were carried out using DockingServer [32]. The MMFF94 force field was used for energy minimization of the ligand molecule using DockingServer [33]. Gasteiger partial charges were added to the ligand atoms. Nonpolar hydrogen atoms were merged, and rotatable bonds were defined.

Docking calculations were carried out on a trypsin protein model (PDB code 2ZQ1). Essential hydrogen atoms, Kollman united atom type charges, and solvation parameters were added with the aid of AutoDock tools [34]. Affinity (grid) maps of $100 \times 100 \times 100$ Å grid points and 0.375 Å spacing were generated using the Autogrid program [34]. The AutoDock parameter set and distance-dependent dielectric functions were used in the

Table 4. The effects of TC (CTC) on the percentage of secondary structural elements in trypsin.

Molar ratio (trypsin to TC (CTC))	Secondary structural elements in trypsin			
	Helix (±0.1%)	Beta (±2%)	Turn (±1%)	Random (±1%)
1:0	1.2	49.5	8.6	40.8
1:1 TC	1.7	42.6	15.6	40.1
1:1 CTC	0.5	54.5	4.8	40.2

doi:10.1371/journal.pone.0028361.t004

calculation of the van der Waals and the electrostatic terms, respectively.

Docking simulations were performed using the Lamarckian genetic algorithm (LGA) and the Solis & Wets local search method [35]. Initial positions, orientations, and torsions of the ligand molecules were set randomly. Each run of the docking experiment was set to terminate after a maximum of 250000 energy evaluations. The population size was set to 150. During the search, a translational step of 0.2 Å, and quaternion and torsion steps of 5 were applied.

Supporting Information

Figure S1 Molecular structure of trypsin (PDB code 2ZQ1). Different types of the secondary structure of trypsin are colour-coded as follows: α -helix: magenta, β -pleated sheet: yellow, β -turn: aquamarine, random coil: white. (TIF)

References

- Chen WR, Huang CH (2010) Adsorption and transformation of tetracycline antibiotics with aluminum oxide. *Chemosphere* 79: 779–785.
- Uslu MO, Balcioglu IA (2009) Comparison of the ozonation and Fenton process performances for the treatment of antibiotic containing manure. *Sci Total Environ* 407: 3450–3458.
- Ye Z, Weinberg HS, Meyer MT (2007) Trace analysis of trimethoprim and sulfonamide, macrolide, quinolone, and tetracycline antibiotics in chlorinated drinking water using liquid chromatography electrospray tandem mass spectrometry. *Anal Chem* 79: 1135–1144.
- Yang M, Xu Y, Wang JH (2006) Lab-on-valve system integrating a chemiluminescent entity and in situ generation of nascent bromine as oxidant for chemiluminescent determination of tetracycline. *Anal Chem* 78: 5900–5905.
- Wei X, Wu SC, Nie XP, Yediler A, Wong MH (2009) The effects of residual tetracycline on soil enzymatic activities and plant growth. *J Environ Sci Health B* 44: 461–471.
- Wollenberger L, Halling-Sorensen B, Kusk KO (2000) Acute and chronic toxicity of veterinary antibiotics to *Daphnia magna*. *Chemosphere* 40: 723–730.
- Hong MZ, Yan QW, Qiu HZ (2010) Fluorimetric study of interaction of benzidine with trypsin. *Journal of Luminescence* 130: 781–786.
- Tucker PC, Webster PD (1972) Effects of tetracycline on pancreatic protein synthesis and secretion in pigeons. *Am J Dig Dis* 17: 675–682.
- Hobusch D, Putzke HP (1971) [Effect of oxytetracycline (OTC) on the secretion kinetics of the rat exocrine pancreas]. *Exp Pathol (Jena)* 5: 298–307.
- Lorenzo C, del Olmo Martinez ML, Pastor L, Almaraz A, Belmonte A, et al. (1999) Effects of oxytetracycline on the rat exocrine pancreas. *Int J Pancreatol* 26: 181–188.
- Imamura T, Matsushita K, Travis J, Potempa J (2001) Inhibition of trypsin-like cysteine proteinases (gingipains) from *Porphyromonas gingivalis* by tetracycline and its analogues. *Antimicrob Agents Chemother* 45: 2871–2876.
- Chi Z, Liu R, Zhang H (2010) Noncovalent interaction of oxytetracycline with the enzyme trypsin. *Biomacromolecules* 11: 2454–2459.
- Yuan T, Weljie AM, Vogel HJ (1998) Tryptophan fluorescence quenching by methionine and selenomethionine residues of calmodulin: orientation of peptide and protein binding. *Biochemistry* 37: 3187–3195.
- Khan SN, Islam B, Yennamalli R, Sultan A, Subbarao N, et al. (2008) Interaction of mitoxantrone with human serum albumin: spectroscopic and molecular modeling studies. *Eur J Pharm Sci* 35: 371–382.
- Zhang YZ, Zhou B, Zhang XP, Huang P, Li CH, et al. (2009) Interaction of malachite green with bovine serum albumin: determination of the binding mechanism and binding site by spectroscopic methods. *J Hazard Mater* 163: 1345–1352.
- Förster T (1965) Delocalized excitation and excitation transfer. In: *Sinanoglu O*, ed. *Modern Quantum Chemistry*. New York: Academic Press. pp 93–137.
- Huang YB, Liu BZ, Yu Z, Zi YQ (2010) Luminescence quenching effect for the interaction of prulifloxacin with trypsin-Britton-Robinson buffer solution system. *Journal of Luminescence* 130: 360–364.
- Zhang B, Xing YH, Li ZW, Zhou HY, Mu QX, et al. (2009) Functionalized Carbon Nanotubes Specifically Bind to α -Chymotrypsin's Catalytic Site and Regulate Its Enzymatic Function. *Nano Letters* 9: 2280–2284.
- Graf L, Jancso A, Szilagyi L, Hegyi G, Pinter K, et al. (1988) Electrostatic complementarity within the substrate-binding pocket of trypsin. *Proc Natl Acad Sci U S A* 85: 4961–4965.
- Ma W, Tang C, Lai L (2005) Specificity of trypsin and chymotrypsin: loop-motion-controlled dynamic correlation as a determinant. *Biophys J* 89: 1183–1193.
- Nilsson MT, Krajewski WW, Yellagunda S, Prabhuramurthy S, Chamarahally GN, et al. (2009) Structural basis for the inhibition of *Mycobacterium tuberculosis* glutamine synthetase by novel ATP-competitive inhibitors. *J Mol Biol* 393: 504–513.
- Yang Q, Liang J, Han H (2009) Probing the interaction of magnetic iron oxide nanoparticles with bovine serum albumin by spectroscopic techniques. *J Phys Chem B* 113: 10454–10458.
- Chi Z, Liu R (2011) Phenotypic characterization of the binding of tetracycline to human serum albumin. *Biomacromolecules* 12: 203–209.
- Wu T, Wu Q, Guan S, Su H, Cai Z (2007) Binding of the environmental pollutant naphthol to bovine serum albumin. *Biomacromolecules* 8: 1899–1906.
- Wang YQ, Zhang HM, Zhang GC, Liu SX, Zhou QH, et al. (2007) Studies of the interaction between paraquat and bovine hemoglobin. *International Journal of Biological Macromolecules* 41: 243–250.
- Hu YJ, Liu Y, Xiao XH (2009) Investigation of the Interaction between Berberine and Human Serum Albumin. *Biomacromolecules* 10: 517–521.
- Yang JT, Wu CS, Martinez HM (1986) Calculation of protein conformation from circular dichroism. *Methods Enzymol* 130: 208–269.
- Shyamali SS, Lillian DR, Lawrence L, Esther B (1979) Fluorescence studies of native and modified neurophysins. Effects of peptides and pH. *Biochemistry* 18: 1026–1036.
- Hossain M, Khan AY, Suresh Kumar G (2011) Interaction of the anticancer plant alkaloid sanguinarine with bovine serum albumin. *PLoS One* 6: e18333.
- Gokara M, Sudhamalla B, Amooru DG, Subramanyam R (2010) Molecular Interaction Studies of Trimethoxy Flavone with Human Serum Albumin. *Plos One* 5: e8834.
- Ghosh S (2008) Interaction of trypsin with sodium dodecyl sulfate in aqueous medium: a conformational view. *Colloids Surf B Biointerfaces* 66: 178–186.
- Bikadi Z, Hazai E (2009) Application of the PM6 semi-empirical method to modeling proteins enhances docking accuracy of AutoDock. *J Cheminform* 1: 15.
- Halgren TA (1998) Merck molecular force field. I. Basis, form, scope, parametrization, and performance of MMFF94. *Journal of Computational Chemistry* 17: 490–519.
- Morris GM, Halliday RS, Huey R, Hart WE, Belew RK, et al. (1998) Automated docking using a Lamarckian genetic algorithm and an empirical binding free energy function. *Journal of Computational Chemistry* 19: 1639–1662.
- Solis EJ, Wets RJB (1981) Minimization by Random Search Techniques. *Mathematics of Operations Research* 6: 19–30.

Figure S2 Plot of $\log [(F_0-F)/F]$ vs $\log [TC (CTC)]$ for the binding of TC and CTC to trypsin at various temperatures.

(TIF)

Figure S3 Overlap of the absorption spectrum of TC and CTC with fluorescence emission spectrum of trypsin (corrected). Conditions: Curve a: the absorption spectrum of TC (CTC); Curve b: the fluorescence emission spectrum of trypsin. The concentration of both TC (CTC) and trypsin are 5×10^{-6} mol L⁻¹.

(TIF)

Author Contributions

Performed the experiments: ZC JW. Analyzed the data: ZC. Contributed reagents/materials/analysis tools: ZC HY HS JW. Wrote the paper: ZC. Designed the experiments: ZC RL. Corrected the paper: RL.